



LAWRENCE
LIVERMORE
NATIONAL
LABORATORY

Distinguishing Pu Metal From Pu Oxide Using Fast Neutron Counting

J. M. Verbeke, G. F. Chapline, L. Nakae, R.
Wurtz, S. Sheets

June 4, 2012

Institute for Nuclear Materials Management
Orlando, FL, United States
July 15, 2012 through July 19, 2012

Disclaimer

This document was prepared as an account of work sponsored by an agency of the United States government. Neither the United States government nor Lawrence Livermore National Security, LLC, nor any of their employees makes any warranty, expressed or implied, or assumes any legal liability or responsibility for the accuracy, completeness, or usefulness of any information, apparatus, product, or process disclosed, or represents that its use would not infringe privately owned rights. Reference herein to any specific commercial product, process, or service by trade name, trademark, manufacturer, or otherwise does not necessarily constitute or imply its endorsement, recommendation, or favoring by the United States government or Lawrence Livermore National Security, LLC. The views and opinions of authors expressed herein do not necessarily state or reflect those of the United States government or Lawrence Livermore National Security, LLC, and shall not be used for advertising or product endorsement purposes.

DISTINGUISHING PU METAL FROM PU OXIDE USING FAST NEUTRON COUNTING

Jérôme M. Verbeke, George F. Chapline, Leslie F. Nakae, Ronald E. Wurtz, Steven A. Sheets
Lawrence Livermore National Laboratory
P.O. Box 808, Livermore, CA 94551

ABSTRACT

We describe a method for simultaneously determining the α -ratio and k_{eff} for fissile materials using fast neutrons. Our method is a generalization of the Hage-Cifarrelli method for determining k_{eff} for fissile assemblies which utilizes the shape of the fast neutron spectrum. In this talk we illustrate the method using Monte Carlo simulations of the fast neutrons generated in PuO_2 to calculate the fast neutron spectrum and Feynman correlations.

INTRODUCTION

Methods based on time-correlated signals have been developed over many years to characterize fissile materials. For example, we can record sequences of thermal neutrons using ^3He tubes or similar neutron detectors, and determine features of the measured object by segmenting the recorded signals into time windows, and counting how many neutrons arrive in each window to build statistical count distributions. Because ^3He tubes only measure thermal neutrons, the high energy neutrons generated by the Pu fission and α -decay cannot be measured immediately, but only after tens of microseconds, which is the time it takes for a fast neutron to thermalize in the moderating material and to eventually be captured by ^3He . Therefore, the time windows must be of the order of tens to hundreds of microseconds to pick up any correlations in the signal. Unfortunately, for strong neutron sources such as Pu, many fission chains will be generated within such long time windows, and the correlation signal will not uniquely consist of single fission chains, but predominantly of several fission chains overlapping in the window. This makes the signal more difficult to extract information out of the measurement.

Liquid scintillators on the other hand, can detect fission neutrons at their initial high energy, because the reaction used for detection is inelastic scattering of neutrons primarily on hydrogen, producing a recoil proton from which scintillation light is promptly produced. In contrast to ^3He tubes which can hardly detect any fast neutrons, liquid scintillators cannot detect any neutrons below 1 MeV, because the recoil proton for such neutrons do not produce enough scintillation light to distinguish them from the light produced by background gamma-ray interactions with the scintillator. At energies above 1 MeV, neutrons travel at a fraction of the speed of light, and can thus be detected within 100 nanoseconds for detection systems of the order of 1 meter in size. One no longer needs to open time windows as long as 100 μs to pick up the correlation signal with ^3He , but only as long as 100 ns. These shorter time windows will greatly reduce the number of overlapping chains within a time window and we will be in a regime where time windows encompass neutrons from single or mostly a few fission chains.

This report describes our efforts to develop algorithms to distinguish plutonium metal from plutonium oxide using liquid scintillators for fast neutron detection. We tested our algorithms using Monte Carlo simulations

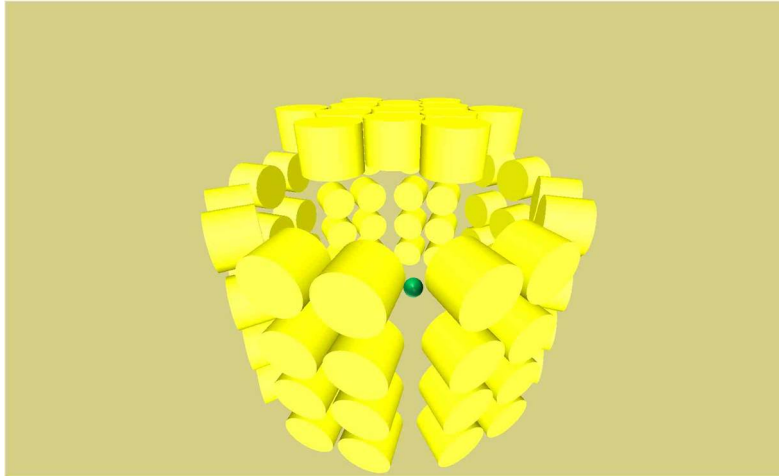


Figure 1: Object in the middle of the 77 liquid scintillator array.

where we assumed that a plutonium metal object is located in the middle of the array of liquid scintillators depicted in Fig. 1. If the object consists of multiplying material, each spontaneous fission can be the source of a fission chain. Particles produced in either the spontaneous fissions or induced fissions of the fission chain travel outward towards the liquid scintillator cells, where they are detected with a known efficiency. Additionally, gamma-rays are emitted as the plutonium α -decays. This source of gamma-rays is many orders of magnitude stronger than the fission gamma-rays.

An important difference between Pu metal and Pu oxide is that PuO₂ is a source of single neutrons emitted randomly. In PuO₂, the alpha particles produced by the α -decay of plutonium carry enough energy — approximately 5 to 5.5 MeV — to cause ¹⁸O to emit a single neutron via an (α ,n) reaction when the α -particle gets to that nucleus. Because of the random nature of the α -decay, single neutrons are thus emitted randomly. These single neutrons are emitted at a rate comparable to the one of spontaneous fission neutrons. Their energy averages 1.9 MeV.

Density is another difference between plutonium metal and plutonium oxide. While the metal has a density of 15.92 g/cm³, the oxide density is only 3 g/cm³.

This knowledge of the differences between the physical properties of the two chemical forms of plutonium will allow us to build algorithms to distinguish them unambiguously.

DESCRIPTION OF PU OBJECTS SIMULATED

To start with, we considered two objects spherical in shape, of identical total weights equal to 5.5366 kg, and of identical outer radii equal to 7.62 cm. This outer radius was chosen such that a plutonium oxide ball of that radius weighs exactly 5.5366 kg. Because plutonium metal has a much higher density, it will form a hollow spherical shell. The complete characteristics of the 2 objects are given in table 1 in terms of geometry, and in table 2 in terms of isotopic composition.

Knowing the neutron yields of the different isotopes (table 3) composing the 2 objects, we calculated that the rate of spontaneous fissions were 158,937 spontaneous fissions/s for the plutonium metal, and 140,170 spontaneous fissions/s for the plutonium oxide.

A large number of gamma-rays are emitted by the α -decay of plutonium. The α -particles emitted by the plutonium α -decay carry between 4.89 and 5.49 MeV depending on the isotope. In the case of PuO₂, if the α -particle hits oxygen, it can cause a (α ,n) reaction. For a 5.2 MeV α -particle incident on a thick oxygen target,

Table 1: Geometric characteristics of the plutonium metal and oxide objects.

Object	Pu metal	Pu oxide
shape	spherical shell	sphere
density [g/cm ³]	15.92	3.
weight [g]	5536.6	5536.6
inner radius [cm]	7.10768	-
outer radius [cm]	7.62	7.62

Table 2: Weights and neutron yields of isotopes composing the Pu metal and PuO₂ objects.

Isotope	Pu metal			PuO ₂		
	weight [g]	yield [n/s]	s.f. yield [s.f./s]	weight [g]	yield [n/s]	s.f. yield [s.f./s]
¹⁶ O	-	-	-	655.0	-	-
¹⁷ O	-	-	-	0.2560	-	-
¹⁸ O	-	-	-	1.320	-	-
²³⁸ Pu	0.7895	2045.	925.3	0.6963	1803.	816.0
²³⁹ Pu	5198.	113.3	52.45	4584.	99.94	46.27
²⁴⁰ Pu	332.1	338741.	156824.	292.9	298743.	138307.
²⁴¹ Pu	27.22	1.36	0.6044	24.01	1.20	0.5335
²⁴² Pu	1.418	2439.	1134.4	1.251	2151.	1000.4
²⁴¹ Am	0.3970	0.4684	0.1455	0.3501	0.4131	0.1283
Total	5536.6	343340.	158937.	5536.6	302799.	140170.

Table 3: Neutron yields of plutonium and americium isotopes of interest.

Isotope	Fission yield [n/s/g]	Spontaneous multiplicity
²³⁸ Pu	2.59E+3	2.21
²³⁹ Pu	2.18E-2	2.16
²⁴⁰ Pu	1.02E+3	2.16
²⁴¹ Pu	5.00E-2	2.25
²⁴² Pu	1.72E+3	2.15
²⁴¹ Am	1.18E+0	3.22

the (α ,n) reaction on oxygen will emit neutrons of mean energy 1.9 MeV, and with a probability of 5.9 neutron producing interactions for every 10⁸ α -particles. The probability of interaction is lower in PuO₂ because of the lower atom fraction of oxygen compared to a thick oxygen target. We can compute the strength of the (α ,n) source using the code SOURCE-4C [3]. The spectrum of the neutrons emitted from the (α ,n) reactions is shown in Fig. 2, their emission rate is 127.1 neutrons/s-cm³. Because liquid scintillators are transparent to neutrons under 1 MeV, it is very important to account for the full energy spectrum of the (α ,n) neutrons, instead just taking the mean energy of 1.9 MeV. Experience shows that assigning the full 1.9 MeV energy to all of the 127.1 neutrons/s-cm³ would result in an artificially inflated efficiency, and an artificially deflated multiplication. For the PuO₂ volume of 1853 cm³, the total emission rate is 235,516 neutrons/s, which is 78% of the rate of neutrons due to spontaneous fissions in plutonium. Another reference [4] gave the values in table 4 for the (α ,n)

neutron yields per gram of plutonium. This table give a total neutron output of 226,254 neutrons/s for our PuO₂ sphere, which is very similar to the values obtained with the code SOURCES-4C. For the purpose of this work, we used the (α ,n) neutron rate given by the code SOURCE-4C.

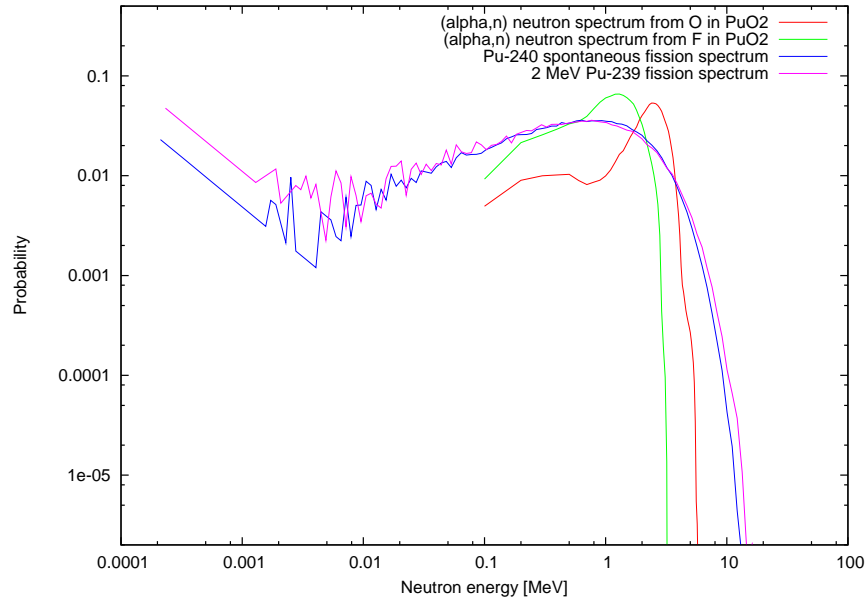


Figure 2: Energy distributions of neutrons from the (α ,n) reactions on O and F in PuO₂, from ²⁴⁰Pu spontaneous fission and from ²³⁹Pu induced fission.

Table 4: (α ,n) neutron yields of isotopes composing the PuO₂ ball, per gram of plutonium.

Isotope	weight [g]	(α ,n) yield [n/s/(g of Pu)]	(α ,n) yield [n/s]
²³⁸ Pu	0.6963	1.9028	9330.304
²³⁹ Pu	4584.	35.62	174661.245
²⁴⁰ Pu	292.9	8.42	41287.133
²⁴¹ Pu	24.01	6.364e-3	31.206
²⁴² Pu	1.251	5.10e-4	2.501
²⁴¹ Am	0.3501	0.192	941.464
Total	4903.	46.14	226254

MOMENT EQUATIONS WITH DIFFERENT MULTIPLICATIONS AND EFFICIENCIES FOR (α, n) NEUTRONS AND FISSION NEUTRONS

Simulations of the 2 objects were performed for a real time of 2 minutes. The times of arrival of the neutrons in each of the liquid scintillator cells were recorded. Randomly splitting the sequence of time tags into N segments of length T — where T is of the order of nanoseconds to hundreds of microseconds —, one can count how many neutrons arrive in the first segment, how many in the second segment, in the third one, etc. and build a distribution $b_n(T)$ of the number n of neutrons arriving in the segments of length T . For the sake of illustration, one such count distribution is shown in Fig. 3. By repeating this procedure for segments of different lengths T , multiple count distributions $b_n(T)$ can be obtained.

These count distributions $b_n(T)$ can be used to determine the strength F_s of the spontaneous fission sources in the object, the efficiency ε of the liquid scintillator array, the multiplication M of the multiplying object, as well as the rate of neutrons from the (α, n) reactions. This will be shown by way of the following three equations for thermal neutron detectors. One can show theoretically, the first moment of the count distribution $b_n(T)$ can be written as

$$\bar{C}(T) = \varepsilon q(M) M \bar{v}_s F_s (1 + \alpha) T \quad (1)$$

where F_s is the strength of the spontaneous fission source in units of spontaneous fissions per second, α is the ratio of neutrons produced by sources emitting single neutrons, to neutrons produced by sources emitting multiple neutrons simultaneously. α is such that $\alpha \varepsilon q(M) M \bar{v}_s F_s T$ is the number of measured neutrons produced by sources emitting single neutrons at a time. $q(M)M$ is usually referred to as the escape multiplication and is given by

$$q(M)M = M - (M - 1)/\bar{v} \quad (2)$$

The symbols \bar{v} and \bar{v}_s are the average numbers of neutrons emitted per induced and spontaneous fissions, respectively. They can be written as $\bar{v} = \sum_{n=1}^8 n C_n$ and $\bar{v}_s = \sum_{n=1}^8 n C_n^s$ where C_n and C_n^s are the probabilities of emitting n neutrons per induced and spontaneous fissions, respectively. The upper limit of 8 on the summation sign is the largest number of neutrons that known isotopes produce per fission. In other words, C_n is zero for n greater than 8. It should be noted that the distribution C_n depends on the energy of the neutron inducing fission.

We see in Fig. 2 that the energies of the neutrons from the reaction (α, n) on oxygen are typically higher than the fission neutron energies. Indeed, the mean fission neutron energy is about 1 MeV while the mean (α, n) neutron energy on oxygen is 2 MeV. This has two effects: (a) the average number of fission neutrons \bar{v}_α due to (α, n) neutrons will be higher than the average number of fission neutrons due to fission neutrons \bar{v} or spontaneous fissions \bar{v}_s , resulting in two different multiplications for the (α, n) neutron initiated fission chains and the spontaneous fission initiated fission chains. (b) The detection efficiencies for (α, n) neutrons ε_α and fission neutrons ε_f will be different as well. One can indeed expect a much higher detection probability for the (α, n) neutrons with a higher mean energy than for the fission neutrons.

To account for this effect, we follow Hage and Cifarelli [5, 6] and rewrite Eq. 1 as

$$\bar{C}(T) = [\varepsilon_f q_f(M_f) [M_f + \alpha (M_\alpha - 1)] \bar{v}_s F_s + \varepsilon_\alpha q_\alpha(M_\alpha) \alpha \bar{v}_s F_s] T \quad (3)$$

where $\varepsilon_f q_f$ and $\varepsilon_\alpha q_\alpha$ are detection efficiencies for fission and (α, n) neutrons, while M_f and M_α are their neutron multiplications. α is the usual parameter specifying the strength of (α, n) neutron emission relative to the rate of neutron emission from spontaneous fission. The efficiencies and neutron multiplication are in general different for fission and (α, n) neutrons because the fission and (α, n) neutrons have different energy spectra. Indeed for the case of PuO_2 the efficiency for detecting the oxygen (α, n) neutrons in our liquid scintillators will

be significantly higher than for fission neutrons, because the energy spectrum for the (α, n) neutrons is peaked around 2 MeV where the intrinsic efficiency of the detector is relatively large, whereas almost half the fission neutrons have energies below 1 MeV where the intrinsic efficiency of our liquid scintillators is very small.

The slope of Eq. 3 is the average count rate

$$R_1 = \varepsilon_f q_f (M_f) [M_f + \alpha (M_\alpha - 1)] \bar{v}_s F_s + \varepsilon_\alpha q_\alpha (M_\alpha) \alpha \bar{v}_s F_s \quad (4)$$

The second and third moments of the $b_n(T)$ distribution, normalized by the count rate, are

$$Y_{2F}(T) = \frac{[\varepsilon_f q_f (M_f) M_f]^2}{\varepsilon_f q_f (M_f) [M_f + \alpha (M_\alpha - 1)] + \alpha \varepsilon_\alpha q_\alpha} [D_{2s} + [(M_f - 1) + \alpha (M_\alpha - 1)] D_2] \left(1 - \frac{1 - e^{-\lambda T}}{\lambda T} \right) \quad (5)$$

$$Y_{3F}(T) = \frac{[\varepsilon_f q_f (M_f) M_f]^3}{\varepsilon_f q_f (M_f) [M_f + \alpha (M_\alpha - 1)] + \alpha \varepsilon_\alpha q_\alpha} [D_{3s} + [(M_f - 1) + \alpha (M_\alpha - 1)] D_3] \left(1 - \frac{3 - 4e^{-\lambda T} + e^{-2\lambda T}}{2\lambda T} \right) \\ + 2 \frac{[\varepsilon_f q_f (M_f) M_f]^3}{\varepsilon_f q_f (M_f) [M_f + \alpha (M_\alpha - 1)] + \alpha \varepsilon_\alpha q_\alpha} (M_f - 1) [D_{2s} D_2 + [(M_f - 1) + \alpha (M_\alpha - 1)] D_2^2] \left(1 - \frac{2 - (2 + \lambda T) e^{-\lambda T}}{\lambda T} \right) \quad (6)$$

where λ is a time constant related to the transport of the neutrons in the measured object and the detection system, D_{2s} , D_2 , D_{3s} and D_3 depend on nuclear data, and are given by $D_{2s} = \frac{\sum_{n=2}^8 \binom{n}{2} C_n^s}{\bar{v}_s}$ and $D_2 = \frac{\sum_{n=2}^8 \binom{n}{2} C_n}{\bar{v}}$, $D_{3s} = \frac{\sum_{n=3}^8 \binom{n}{3} C_n^s}{\bar{v}_s}$ and $D_3 = \frac{\sum_{n=3}^8 \binom{n}{3} C_n}{\bar{v}}$.

Because the fission cross-section is fairly flat across all the energies of interest, the neutron multiplications for fission and (α, n) neutrons are nearly the same. Therefore in the following we will set $M_\alpha = M_f \equiv M$. This system of equations 4 through 6 has 5 unknown parameters: M , $\varepsilon_f q_f$, $\varepsilon_\alpha q_\alpha$, α , F_s .

Defining R_{2F} and R_{3F} as the asymptotical values of $Y_{2F}(T)$ and $Y_{3F}(T)$, and following Cifarelli-Hage, we can contemplate writing the ratio R_{3F}/R_{2F}^2 to determine the multiplication M :

$$\frac{R_{3F}}{R_{2F}^2} = \frac{2(M-1)D_2 [D_{2s} + (1+\alpha)(M-1)D_2] + D_{3s} + (1+\alpha)(M-1)D_3}{[D_{2s} + (1+\alpha)(M-1)D_2]^2} \left(\frac{R_1}{\varepsilon_f q M \bar{v}_s F_s} \right) \quad (7)$$

Unfortunately, we cannot use expression 7 directly to determine the multiplication because of the presence of too many unknown parameters: M , α , ε_f , and ε_α .

We can replace the two efficiencies by a single parameter by making use of the theoretical fission and (α, n) spectra shown in Fig. 2 to calculate the ratio $\varepsilon_\alpha/\varepsilon_f$. Calling this ratio r_ε we have

$$\frac{R_{3F}}{R_{2F}^2} = \frac{2(M-1)D_2 [D_{2s} + (1+\alpha)(M-1)D_2] + D_{3s} + (1+\alpha)(M-1)D_3}{[D_{2s} + (1+\alpha)(M-1)D_2]^2} \left[\left[1 + \alpha \left(\frac{M-1}{M} \right) \right] + r_\varepsilon \frac{\alpha}{M} \right] \quad (8)$$

The efficiency ratio r_ε depends on the theoretical fission and (α, n) neutron spectra and the characteristics of the neutron detector. For our liquid scintillators we find $r_\varepsilon \sim 1.602$. Given a value for r_ε one can in principle use Eq. 8 to solve for the multiplication as a function of α . Unfortunately this equation is now a cubic equation rather than the quadratic equation in the $\alpha = 0$ case considered by Cifarelli and Hage.

As an alternative we can use the observed spectrum to directly evaluate the quantity $\left[1 + \alpha \left(\frac{M-1}{M} \right) \right] + r_\varepsilon \frac{\alpha}{M}$ in Eq. 8. In particular, fitting the observed fast neutron spectrum to a sum of fission and (α, n) spectra yields

two coefficients whose ratio ρ should be equal to $\frac{r_\epsilon \alpha}{M + \alpha(M-1)}$. Given this additional experimental input, one can rewrite Eq. 8 as

$$\frac{R_{3F}}{R_{2F}^2} = \frac{2(M-1)D_2[D_{2s} + (1+\alpha)(M-1)D_2] + D_{3s} + (1+\alpha)(M-1)D_3}{[D_{2s} + (1+\alpha)(M-1)D_2]^2} \left[1 + \alpha \left(\frac{M-1}{M} \right) \right] (1+\rho) \quad (9)$$

Using the definition of ρ , we can write the following relationship between α and M :

$$\alpha = \frac{M}{\frac{r_\epsilon}{\rho} - M + 1} \quad (10)$$

In the limit of small ρ , $\alpha \rightarrow \frac{\rho}{r_\epsilon}$, while in the limit of large α , $\rho \rightarrow \frac{r_\epsilon}{M-1}$. Substituting Eq. 10 into 9, we find that α becomes the solution of the following quadratic equation:

$$2D_2 \left(\frac{\alpha r_\epsilon}{\rho} - 1 \right) \left[D_{2s} + \left(\frac{\alpha r_\epsilon}{\rho} - 1 \right) D_2 \right] + (1+\alpha) \left[D_{3s} + \left(\frac{\alpha r_\epsilon}{\rho} - 1 \right) D_3 \right] = \frac{1 + \frac{\rho}{r_\epsilon} \frac{R_{3F}}{R_{2F}^2}}{1 + \rho} \left[D_{2s} + \left(\frac{\alpha r_\epsilon}{\rho} - 1 \right) D_2 \right]^2 \quad (11)$$

In the next sections, we show that this equation together with the spectral information in the liquid scintillators can be used to solve for the α ratio and the multiplication.

LIQUID SCINTILLATOR TIME CORRELATION RESULTS

Monte-Carlo simulation results for the count distribution for $T=1 \mu\text{s}$, and the 2 moments $Y_{2F}(T)$ and $Y_{3F}(T)$ are shown in Fig. 3 for the Pu metal sphere. The total time is shared among the 10 time gates in such a way as to keep the errors on the $Y_{2F}(T)$ values for the 10 different time gates approximately equal. Fast neutron counts are not re-used among different time gates. The simulation corresponds to a measurement of 2 minutes, 55.23 s contributed to the $1 \mu\text{s}$ time gate, and the remaining 64.77 s were shared between the 9 other time gates. Fig. 4 shows the results for the PuO_2 sphere.

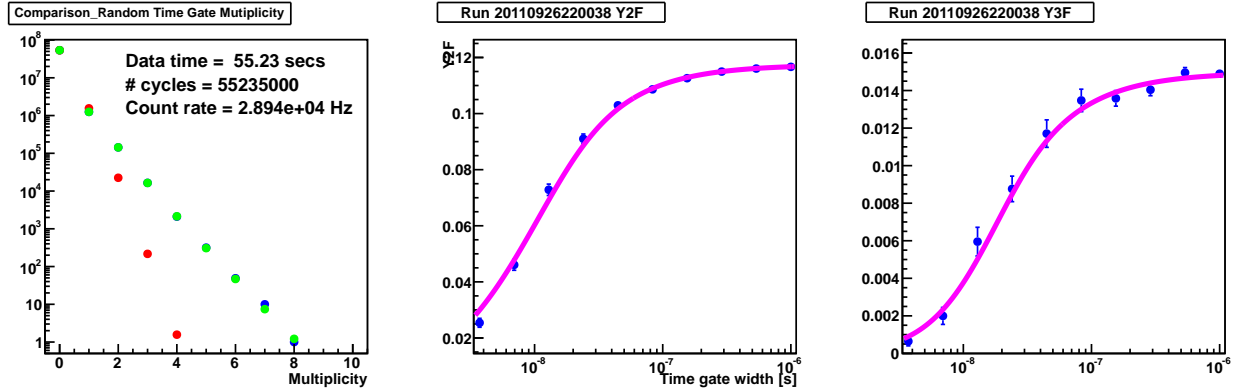


Figure 3: Count distribution $b_n(T)$ for the $1 \mu\text{s}$ time gate, $Y_{2F}(T)$ and $Y_{3F}(T)$ for the Pu metal spherical shell and T between 3 ns and $1 \mu\text{s}$, along with their theoretical reconstructions in light green and magenta. The set of parameters used for the reconstructions is $(M, \epsilon_f, \alpha) = (1.38, 6.9\%, 0.00)$.

LIQUID SCINTILLATORS SPECTRAL INFORMATION

In this section, we show that in principle the information contained in the spectrum of energies deposited by the fast neutrons in the liquid scintillator cells can be used to differentiate plutonium metal from plutonium

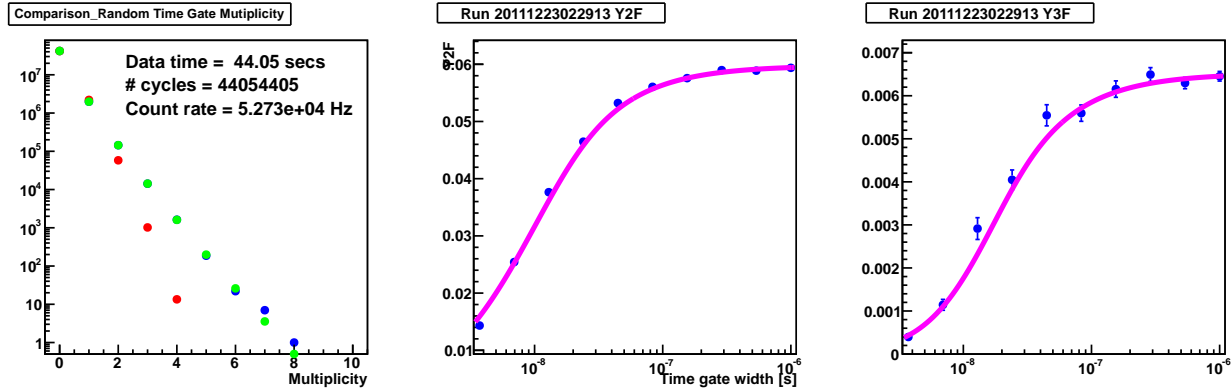


Figure 4: Count distribution $b_n(T)$ for the $1 \mu\text{s}$ time gate, $Y_{2F}(T)$ and $Y_{3F}(T)$ for the Pu oxide ball and T between 3 ns and $1 \mu\text{s}$, along with their theoretical reconstructions in light green and magenta. The set of parameters used for the reconstructions is $(M, \epsilon_f, \alpha) = (1.38, 5.8\%, 0.75)$.

dioxide. Fig. 5 shows the spectra for simulations corresponding to two different neutron sources. The spectrum in red is due to a trace amount of ^{240}Pu producing spontaneous fissions, while the spectrum in blue is due to plutonium generated α -decay particles interacting with oxygen in PuO_2 . One observes that the spectra of energies deposited are significantly different. As shown in Fig. 2, the neutron spectrum for spontaneous fission of ^{240}Pu is similar to the neutron spectrum for induced fission of ^{239}Pu .

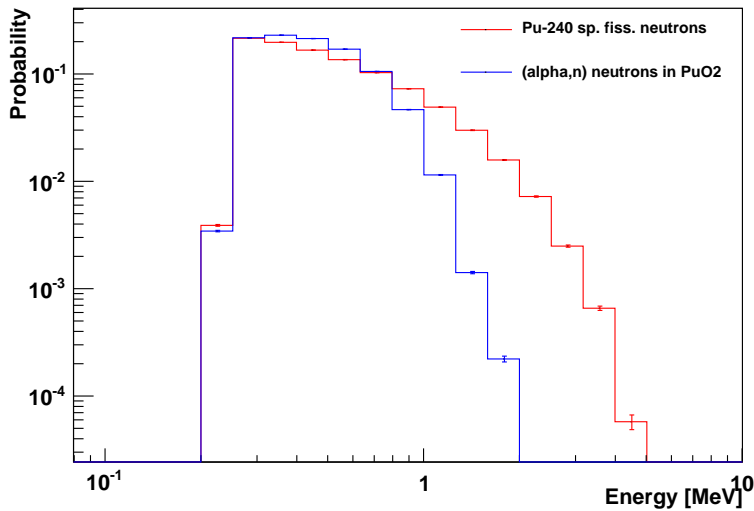


Figure 5: Distributions of energies deposited by the fast neutrons in the liquid scintillator cells for two different neutron sources, (i) ^{240}Pu (red) and (ii) (α, n) neutrons produced in PuO_2 (blue).

For the PuO_2 ball described in tables 1 and 2, the spectrum of energies deposited by the fast neutrons is shown in blue in Fig 6(b). One can add the two spectra shown in Fig. 5 with appropriate weights to reconstruct the blue curve in Fig. 6(b). The optimal combination of weights is given in Fig. 6(a). By adding the ^{240}Pu spectrum pre-multiplied by 0.58 to the (α, n) spectrum pre-multiplied by 0.42, one obtains the reconstruction spectrum of energies deposited shown in red in Fig. 6(b). On the contrary, when one measures the Pu metal

shell, the weights that are optimal for the reconstruction of the spectrum of deposited energies are 0.9986 of the ^{240}Pu spectrum and 0.0014 of the (α,n) spectrum. So it seems that just measuring the spectra of energies deposited by fast neutrons is sufficient to distinguish Pu metal and Pu oxide.

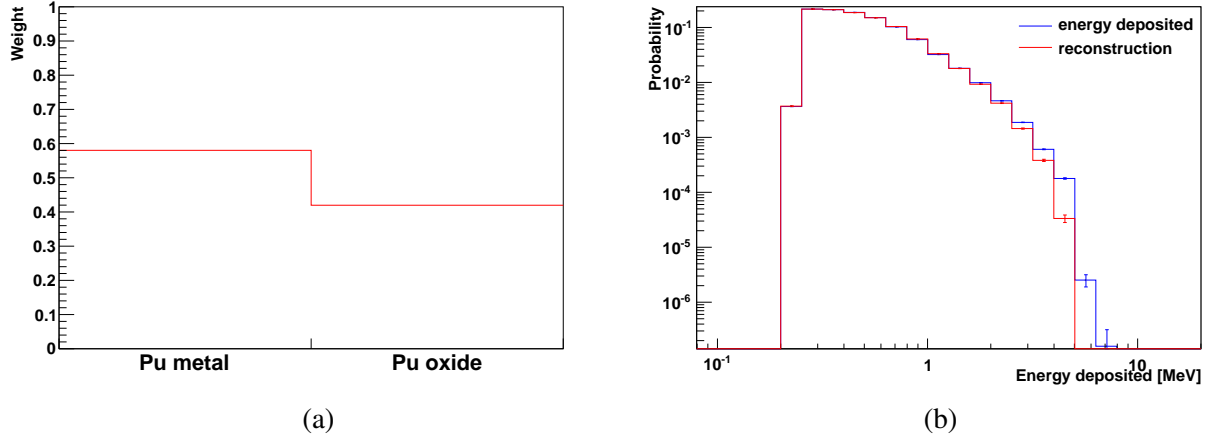


Figure 6: (a) Factors by which the two spectra shown in Fig. 5 must be multiplied to reconstruct the spectrum of energies deposited by the fast neutrons emitted by the PuO_2 ball: 0.58 for the ^{240}Pu spectrum and 0.42 for the (α,n) spectrum. (b) Spectrum of energies deposited by fast neutrons in liquid scintillator cells for the PuO_2 ball (blue), along with its reconstruction (red) from the two spectra shown in Fig. 5 and the optimal weights aside.

Setting $\rho=0.72$, the solution to Eqs. 10-11 with $M \geq 1$ is $\alpha=0.75$, $M=1.38$. Our solution for α is very close to the exact value 0.78. Using Eq. 5, we can determine the value of ϵ_f to be 5.8%, while Eq. 3 implies a spontaneous fission source rate of 345,000 neutrons/sec. Although not exactly the same strength as the value of 302,799 given in table 2, this method gives a result within 15% of the correct answer. For the plutonium metal shell, we find that the fitting algorithm gives $\rho=0.0014$. The solution to Eqs. 10-11 with $M \geq 1$ is $\alpha=0.0012$, $M=1.38$. The value of ϵ_f is 6.9% and the source strength is 332,000 neutrons/sec, which is off by less than 4%.

CONCLUSION

In this report, we have shown first of all that measuring the energy spectrum of the fast neutrons in the liquid scintillators allows one to distinguish the two chemical forms of plutonium. In addition, combining this information with the Feynman 2-neutron and 3-neutron correlations allows one to extract the α -ratio without explicitly knowing the multiplication. Given the α -ratio one can then extract the multiplication as well as the ^{239}Pu and ^{240}Pu masses directly from the moment equations.

ACKNOWLEDGMENTS

This work performed under the auspices of the U.S. Department of Energy by Lawrence Livermore National Laboratory under Contract DE-AC52-07NA27344.

References

- [1] J. M. Verbeke, G. F. Chapline, “Distinguishing plutonium metal from plutonium oxide,” LLNL-TR-518451, Lawrence Livermore National Laboratory (2011).
- [2] I. Pázsit, L. Pál, “Neutron Fluctuations, A Treatise on the Physics of Branching Processes,” Elsevier (2008).
- [3] W.B. Wilson, R.T. Perry, E.F. Shores, W.S. Charlton, T.A. Parish, G.P. Estes, T.H. Brown, E.D. Arthur, M. Bozoian, T.R. England, D.G. Madland, and J.E. Stewart, “SOURCES 4C: A Code for Calculating (α ,n), Spontaneous Fission, and Delayed Neutron Sources and Spectra,” LA-UR-02-1839, Los Alamos National Laboratory (2002).
- [4] Private communication with Les Nakae, September 2011.
- [5] W. Hage, D.M. Cifarelli, “Correlation Analysis with Neutron Count Distributions in Randomly or Signal Triggered Time Intervals for Assay of Special Fissile Materials,” *Nucl. Sci. and Eng.* **89**, 159-176 (1985).
- [6] D.M. Cifarelli, W. Hage, “Models for a Three-Parameter Analysis of Neutron Signal Correlation Measurements for Fissile Material Assay,” *Nucl. Instr. and Meth. in Phys. Res.* **A251**, 550-563 (1986).